Equivalent Circuit Allowing Loss Separation Synthesized from Field Computations: Application to Induction Heating

Toshihito Shimotani[1,2], Hajime Igarashi[2], Eiji Hashimoto[1], Hiroyuki Imanari[1], *Member IEEE*

[1]Toshiba Mitsubishi-Electric Industrial Systems Corporation (TMEIC), 3-1-1 Kyobashi, Chuo-ku, Tokyo Japan,
[2]Information Science and Technology Department, Hokkaido University, Kita 14, Nishi 9, Sapporo, Hokkaido, Japan

This paper presents a method to synthesize the equivalent circuit of an induction heating (IH) machine used in hot strip mill (HSM) process. The equivalent circuit allows us not only to evaluate eddy current losses in different forms such as iron plate and coils but also compute the transient responses in online environments. The frequency characteristic of the IH machine is effectively computed by proper orthogonal decomposition. The equivalent circuit of the IH is synthesized through curve fitting to the computed characteristics in conjunction with Tikhonov's regularization. The equivalent circuit is shown to have good accuracy and works much faster than the finite element method. The proposed equivalent circuit is expected to be used in online control of the HSM process.

***Index Terms*— Cauer circuit, induction heating, Tikhonov's regularization, genetic algorithm, eddy current loss.**

I. Introduction

In the hot strip mill (HSM) process, the requirement to produce steel sheets with higher strength and lower thickness has become increasingly important in recent years. Temperature control is one of most important factors to make high strength steel because mechanical properties of the steel highly depend on its temperature. Recently, Induction Heaters (IH) have been widely installed in HSM plants for temperature control [1]. Because an IH provides fast and efficient heating for steel plate with rapid control response, it can improve the performance of the HSM process. For this reason, it is strongly desired to develop an accurate and fast IH mathematical model which can be used in online HSM process control.

Fast computing methods for the eddy current problems have been studied [e.g. 2-5]. Proper orthogonal decomposition (POD) [6] is a fast method that generates basis vectors via singular value decomposition to produce a reduced model of field phenomena. A method to synthesize the equivalent circuit of electromagnetic (EM) machines from a finite element (FE) model based on POD has been proposed [2, 3]. The input impedance of an electric machine can be accurately computed using its equivalent circuit derived by POD. However, the conventional method cannot separately evaluate losses in the steel piece (which heats the piece) and losses in the induction heater itself (which do not heat the piece)

In this paper, we propose a new method to synthesize the equivalent circuit which can separately evaluate the losses in the different electromagnetic components of the system i.e., the steel piece and the induction heater. In the proposed method, the circuit parameters are determined by curve fitting in such a way that the frequency characteristics of the impedance and losses effectively computed by POD are consistent with those of the circuit. The real-coded genetic algorithm (RGA) is adopted for curve fitting in conjunction with Tikhonov's regularization for uniqueness of the circuit parameters. The proposed method is applied to a simplified 3D FE model of IH machine, then numerical results are compared with those obtained by the conventional FE analysis (FEA) with respect to the numerical accuracy and computing time.

II. Numerical Method

A. Finite element equation

Let us consider a quasi-static EM field in the frequency domain governed by

$$\mathrm{rot}(\nu\,\mathrm{rot}\boldsymbol{A}) + \sigma(\mathrm{j}\omega\boldsymbol{A} + \mathrm{grad}\varphi) = 0 \quad (1a)$$
$$\mathrm{div}\,\sigma(\mathrm{j}\omega\boldsymbol{A} + \mathrm{grad}\varphi) = 0 \quad (1b)$$

where ν: magnetic resistivity $\boldsymbol{A}$: magnetic vector potential, ω : angular frequency, σ : electrical conductivity, φ : magnetic scalar potential. We consider the external circuit equation coupled with (1a) and (1b) as follows:

$$RI + \mathrm{j}\omega LI = V_{in} \quad (1c)$$

where R : resistance, I : current, L : inductance, V_{in} : input voltage. For FEA, $\boldsymbol{A}$ and φ are discretized in each finite element as follows:

$$\boldsymbol{A} = \textstyle\sum_i a_i \boldsymbol{N}_i,\ \varphi = \sum_k \varphi_k N_k \quad (2a), (2b)$$

where a_i : line integral of d$\boldsymbol{A}$ along ith-edge of the element, φ_k : φ at kth-node of the element, $\boldsymbol{N}_i$: interpolation function for the edge-element, N_k : interpolation function for the node-element. Here, we adopt the formulation proposed in [7] in order to consider eddy currents in the induction coil for IH. Assuming that φ is constant on the arbitrary cross-section of the induction coil, φ is expressed on the inflow surface Γ_{in} of the current in each induction coil as

$$\varphi = \varphi_0 \sum_{\Gamma_{in} \in n} N_n \quad (2c)$$

The FE discretization of (1) based on (2) results in

$$\mathrm{K}\boldsymbol{x} + \mathrm{j}\omega\mathrm{N}\boldsymbol{x} = \boldsymbol{b}V_{in} \quad (3)$$

where

$$\mathrm{K}=\begin{bmatrix}\mathrm{B} & 0 & \mathrm{C} & 0\\ 0 & 0 & 0 & 0\\ \mathrm{C^t} & 0 & 0 & \frac{-1}{\mathrm{j}\omega}\\ 0 & 0 & \frac{-1}{\mathrm{j}\omega} & \frac{-R-\mathrm{j}\omega L}{\mathrm{j}\omega}\end{bmatrix},\ \mathrm{N}=\begin{bmatrix}\mathrm{D} & \mathrm{E} & 0 & 0\\ \mathrm{E^t} & \mathrm{F} & 0 & 0\\ 0 & 0 & \frac{\mathrm{F}}{\mathrm{j}\omega} & 0\\ 0 & 0 & 0 & 0\end{bmatrix},\ \boldsymbol{b}=\begin{bmatrix}0\\ \vdots\\ 0\\ \frac{-V_{in}}{\mathrm{j}\omega}\end{bmatrix} \tag{4}$$

and K, N $\in R^{n\times n}$: FE matrices, $\boldsymbol{x}\in R^n$: solution vector, $\boldsymbol{b}\in R^n$ source vector. The entities in (4) are given by

$$\begin{aligned}
\mathrm{B} &= \sum_i a_i \int_\Omega \mathrm{rot}\boldsymbol{N}_j \cdot \nu \mathrm{rot}\boldsymbol{N}_i\, dV\\
\mathrm{C} &= \varphi_0 \int_\Omega \sigma \cdot \sum_{\Gamma_{in}\in k} \mathrm{grad}N_k\, dV\\
\mathrm{D} &= \mathrm{j}\omega \sum_i a_i \int_\Omega \sigma \boldsymbol{N}_i \cdot \boldsymbol{N}_j dV\\
\mathrm{E} &= \mathrm{j}\omega\varphi_0 \int_\Omega \sigma \boldsymbol{N}_j \cdot \sum_{\Gamma_{in}\in n} \mathrm{grad}N_n\, dV\\
\mathrm{F} &= \mathrm{j}\omega\varphi_0 \int_\Omega \sigma \sum_{\Gamma_{in}\in k} \mathrm{grad}N_k \cdot \sum_{\Gamma_{in}\in n} \mathrm{grad}N_n\, dV
\end{aligned} \tag{5}$$

where Ω means whole analysis region.

B. *Proper Orthogonal Decomposition*

To reduce computing time to solve (3), we employ POD in order to reduce the system (3). Firstly, we solve (3) at s (<<n) different frequencies to take the snapshot $\boldsymbol{x}$ of the EM fields for construction of the data matrix X defined by

$$\mathrm{X} = [\boldsymbol{x}(\omega_1), \boldsymbol{x}(\omega_2), \cdots, \boldsymbol{x}(\omega_s)] \tag{6}$$

Then, singular value decomposition is applied to X to obtain

$$\mathrm{X} = \mathrm{W\Sigma V^*} = \sigma_1 w_1 v_1^* + \sigma_2 w_2 v_2^* + \cdots + \sigma_s w_s v_s^* \tag{7}$$

where * denotes complex conjugate, σ_i : singular values of X in descending order ($\sigma_1 \ge \sigma_2 \ge \ldots$), w_i : eigenvector of XX*, and v_i : eigenvector of X*X. When σ_{r+1} is much smaller than σ_1, X can be approximated as

$$\mathrm{X} \approx \mathrm{X}_r = \sigma_1 w_1 v_1^* + \sigma_2 w_2 v_2^* + \cdots + \sigma_r w_r v_r^* \tag{8}$$

Now $\boldsymbol{x}$ is approximately expressed as a linear combination of w_i, that is, $\boldsymbol{x}$=W$\boldsymbol{x}_r$, where $\boldsymbol{x}_r \in \mathbb{C}^r$. Finally, (3) is reduced to

$$\mathrm{W^*KW}\boldsymbol{x}_r + \mathrm{j}\omega \mathrm{W^*NW}\boldsymbol{x}_r = \mathrm{W^*}\boldsymbol{b}v_{in} \tag{9}$$

It is remarked that (9) can be solved much faster than (3) because r<<n. Therefore, we can obtain the frequency characteristics quickly by solving (9) instead of (3).

C. *Circuit synthesis*

We employ the Cauer circuit [8] shown in Fig.1 as the equivalent circuit of an IH machine. It has been shown that the Cauer-circuit has an advantage that it can represent not only the effect of eddy currents but also non-linear characteristics due to magnetic saturation [9]. However, the original Cauer circuit cannot allow us to separate eddy current losses in different components. In order to evaluate the losses in a steel plate and induction coils separately, we propose a modified Cauer circuit as shown in Fig. 2. We assume that $\boldsymbol{R}_1$=[$R_{1,1}$, …, $R_{q,1}$] and $\boldsymbol{R}_2$=[$R_{1,2}$, …, $R_{q,2}$] represent the DC and AC resistances of the steel plate and induction coils, respectively.

To determine the circuit parameters in Fig. 2, we solve the optimization problem defined by

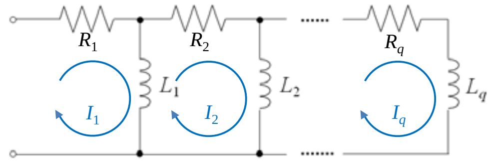

Fig. 1. Conventional Cauer circuit

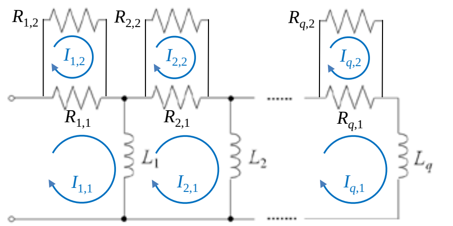

Fig. 2. Modified Cauer circuit proposed in this work

$$\begin{gathered} f(\omega_i, \boldsymbol{R}, \boldsymbol{L}) = \sqrt{\varepsilon_Z + \varepsilon_{W_s} + \varepsilon_{W_c} + \alpha\varepsilon_\alpha} \to \min\\ \text{sub. to } R_j,\ L_j \ge 0 \end{gathered} \tag{10}$$

where

$$\begin{aligned}
\varepsilon_Z &= \frac{\sum_i^m \{Z^{\mathrm{POD}}(\omega_i) - Z^{\mathrm{Cauer}}(\omega_i, \boldsymbol{R}, \boldsymbol{L})\}^2}{\sum_i^m \{Z^{\mathrm{POD}}(\omega_i)\}^2}\\
\varepsilon_{W_s} &= \frac{\sum_i^m \{W_s^{\mathrm{POD}}(\omega_i) - W_s^{\mathrm{Cauer}}(\omega_i, \boldsymbol{R}, \boldsymbol{L})\}^2}{\sum_i^m \{W_s^{\mathrm{POD}}(\omega_i)\}^2}\\
\varepsilon_{W_c} &= \frac{\sum_i^m \{W_c^{\mathrm{POD}}(\omega_i) - W_c^{\mathrm{Cauer}}(\omega_i, \boldsymbol{R}, \boldsymbol{L})\}^2}{\sum_i^m \{W_c^{\mathrm{POD}}(\omega_i)\}^2}\\
\varepsilon_\alpha &= \sum_j^{2q} R_j^2 + \sum_j^q L_j^2\\
Z^{\mathrm{Cauer}} &= R_1 + \cfrac{1}{\mathrm{j}\omega L_1 + \cfrac{1}{(R_{2,1} + \cdots + R_{2,m}) + 1/\mathrm{j}\omega L_2 \cdots}}\\
W_s^{\mathrm{Cauer}}(\omega_i, \boldsymbol{R}, \boldsymbol{L}) &= \sum_{j=1}^q \frac{R_{j,1}(I_{j,1} - I_{j,2})^2}{2}\\
W_c^{\mathrm{Cauer}}(\omega_i, \boldsymbol{R}, \boldsymbol{L}) &= \sum_{j=1}^q \frac{R_{j,2} I_{j,2}^2}{2}
\end{aligned} \tag{11}$$

where $(\omega_i, \boldsymbol{R}, \boldsymbol{L})$: objective function, m : number of the sampling frequencies, Z : impedance, W_s and W_c : losses in steel plate and induction coils. The quantities suffixed with "Cauer" are evaluated by the modified Cauer circuit, while others are computed by solving (9). Moreover, q : number of circuit stages, $\boldsymbol{R}$=[$\boldsymbol{R}_1$, $\boldsymbol{R}_2$] and $\boldsymbol{L}$=[L_1, …, L_q] : arrays that consist of the resistances and inductances of the modified Cauer circuit. In addition, $\alpha\varepsilon_\alpha$ is Tikhonov's regularization term to impose uniqueness in the identification. We adopt the L-curve method [10] to determine the regularization parameter α in by plotting the residual norm r_{norm} against the solution norm s_{norm} by changing the value of α, then adopting α at the corner point of the L curve which gives a good balance. In this problem, r_{norm} and s_{norm} are calculated as follows:

$$r_{norm} = \sqrt{\varepsilon_Z + \varepsilon_{W_s} + \varepsilon_{W_c}} \tag{12}$$

$$s_{norm} = \sqrt{\varepsilon_\alpha} \tag{13}$$

To solve (10), we employ an RGA with conditions as summarized in TABLE I.

TABLE I CONDITIONS FOR RGA

Selection method	RGA
Crossover method	Just Generation Gap (JGG)
Number of the individuals	$60\times q$
Threshold value for convergence	1.0×10^{-8}
MAX number of generations	1.0×10^{5}

III. NUMERICAL RESULTS

The proposed method is applied to a simplified 3D FE model of an IH machine shown in Fig. 3. Considering the spatial symmetry, we only need to model 1/8 of the whole system. The steel plate is transported in the rolling direction and is heated up by eddy currents induced by the AC current in the coils. The iron core strengthens the magnetic flux. The magnetic permeability of the steel plate is assumed to be linear because its temperature is higher than the Curie temperature when the plate passes through this machine in the HSM process. Furthermore, for simplicity, it is assumed that the magnetic saturation in iron core is negligible (although it can be modelled with the Cauer circuit as shown in [9] by changing the value of L_1 in the circuit dynamically depending on the current considering magnetic characteristics).

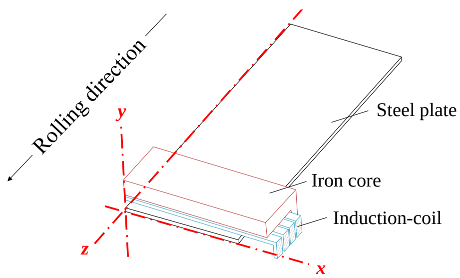

Fig. 3. IH machine (1/8 symmetric model).

A. POD result

Firstly, POD is applied to analyze the IH machine in order to produce a reduced FE equation under the conditions summarized in TABLE II.

TABLE II CONDITIONS FOR SNAPSHOT OF EM FIELDS

Number of snapshot s	Value of r
5 (10, 100, 500, 1000, 1500Hz)	5

The numerical error of the reduced FE equation defined by

$$Error = \sqrt{\frac{\sum_i^n \left|\dot{\boldsymbol{x}}_i^{FEM} - \dot{\boldsymbol{x}}_i^{POD}\right|^2}{\sum_i^n \left|\dot{\boldsymbol{x}}_i^{FEM}\right|^2}} \tag{14}$$

is plotted against frequency in Fig. 4, where $\dot{\boldsymbol{x}}_i^{FEM}$, $\dot{\boldsymbol{x}}_i^{POD}$ are the solution vector $\boldsymbol{x}$ at sampling frequencies obtained by solving the original and reduced FE equations, respectively. Because the numerical error of the reduced FE equation is less than 0.1%, the frequency characteristic of the IH machine is evaluated effectively at arbitrary frequencies in our range of interest by solving (9). Computing time to solve the reduced FE equation is about 5% of that to solve the original one.

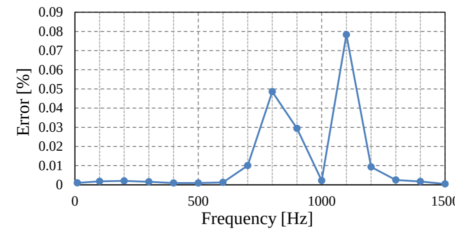

Fig. 4. Numerical error of the POD

B. Determination of regularization parameter

In order to determine the regularization parameter α in (10) for equivalent circuit synthesis, we execute circuit-parameter identification by changing the value of α for the three-stage circuit to obtain the L curve shown in Fig. 5. Referring to the corner point of the L curve, the value of α is set to be 1.0×10^{-3}.

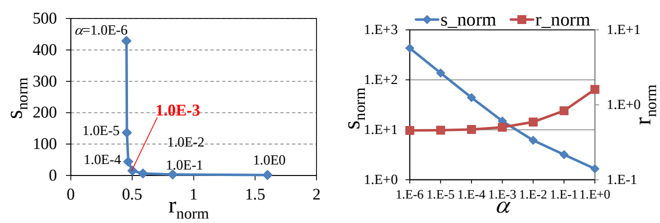

(a) L curve (b) Dependence of norms on α

Fig. 5. Determination of regularization parameter α from L curve (q=3)

C. Circuit parameter

Based on the results in sub-sections III A and B, the circuit shown in Fig.2 is synthesized by the proposed method under the conditions summarized in TABLE III.

TABLE III CONDITIONS FOR CIRCUIT SYNTHESIS

Number of frequency points of input data m	Number of circuit stages q
16 (10, 100, 200, …, 1500Hz)	2, 3, 4

The resultant circuit parameters and the corresponding value of the objective function $f(\omega_i, \boldsymbol{R}, \boldsymbol{L})$ when q=2, 3, 4 are shown in TABLE IV. For each q, five different circuits are synthesized changing initial individuals in the RGA in order to test the uniqueness in the parameters.

TABLE IV CIRCUIT PARAMETERS

(a) q=2

Element [Ω]or[H]	circuit 1	circuit 2	circuit 3	circuit 4	circuit 5
$R_{1,1}$	3.153E+00	3.153E+00	3.153E+00	3.153E+00	3.153E+00
$R_{1,2}$	3.203E-04	3.203E-04	3.203E-04	3.203E-04	3.203E-04
$R_{2,1}$	3.750E-01	3.750E-01	3.750E-01	3.750E-01	3.750E-01
$R_{2,2}$	1.994E+00	1.994E+00	1.994E+00	1.994E+00	1.994E+00
L_1	6.963E-06	6.963E-06	6.963E-06	6.963E-06	6.963E-06
L_2	4.871E-05	4.871E-05	4.871E-05	4.871E-05	4.871E-05
$f(\omega_i,\boldsymbol{R},\boldsymbol{L})$	**8.143E-01**	**8.143E-01**	**8.143E-01**	**8.143E-01**	**8.143E-01**

(b) q=3

Element [Ω]or[H]	circuit 1	circuit 2	circuit 3	circuit 4	circuit 5
$R_{1,1}$	2.062E-01	2.062E-01	2.063E-01	2.062E-01	2.063E-01
$R_{1,2}$	2.115E-04	2.115E-04	2.115E-04	2.115E-04	2.115E-04
$R_{2,1}$	8.161E-01	8.161E-01	8.161E-01	8.163E-01	8.160E-01
$R_{2,2}$	1.312E-02	1.312E-02	1.312E-02	1.312E-02	1.312E-02
$R_{3,1}$	3.632E-01	3.632E-01	3.632E-01	3.632E-01	3.632E-01
$R_{3,2}$	1.492E+01	1.492E+01	1.492E+01	1.492E+01	1.492E+01
L_1	7.922E-06	7.922E-06	7.922E-06	7.922E-06	7.922E-06
L_2	5.004E-05	5.004E-05	5.004E-05	5.004E-05	5.004E-05
L_3	5.371E-05	5.371E-05	5.371E-05	5.371E-05	5.371E-05

$f(\omega_i,\boldsymbol{R},\boldsymbol{L})$	**2.839E-01**	**2.839E-01**	**2.839E-01**	**2.839E-01**	**2.839E-01**

(c) q=4

Element [Ω]or[H]	circuit 1	circuit 2	circuit 3	circuit 4	circuit 5
$R_{1,1}$	2.062E-01	2.063E-01	2.063E-01	2.064E-01	2.063E-01
$R_{1,2}$	2.115E-04	2.115E-04	2.115E-04	2.115E-04	2.115E-04
$R_{2,1}$	8.163E-01	8.161E-01	8.160E-01	8.158E-01	8.158E-01
$R_{2,2}$	1.312E-02	1.312E-02	1.312E-02	1.312E-02	1.312E-02
$R_{3,1}$	3.632E-01	3.632E-01	3.632E-01	3.632E-01	3.632E-01
$R_{3,2}$	1.492E+01	1.492E+01	1.492E+01	1.492E+01	1.492E+01
$R_{4,1}$	1.484E-04	2.739E-04	2.646E-05	1.417E-04	2.768E-04
$R_{4,2}$	2.389E-13	8.845E-12	1.007E-03	2.091E-11	5.870E-08
L_1	7.922E-06	7.922E-06	7.922E-06	7.922E-06	7.922E-06
L_2	5.004E-05	5.004E-05	5.004E-05	5.004E-05	5.004E-05
L_3	3.064E-04	3.242E-04	5.397E-05	6.796E-04	5.514E-05
L_4	6.513E-05	6.437E-05	1.103E-02	5.832E-05	2.077E-03
$f(\omega_i,\boldsymbol{R},\boldsymbol{L})$	**2.839E-01**	**2.839E-01**	**2.839E-01**	**2.839E-01**	**2.839E-01**

When q=2, there are no differences in the circuit parameters among the trials of RGA. When q=3, there are again almost no differences in them and $f(\omega_i,\boldsymbol{R},\boldsymbol{L})$ takes smaller values in comparison with those in q=2. When q=4, the parameters in the front stages are almost the same as those when q=3 and $f(\omega_i,\boldsymbol{R},\boldsymbol{L})$ takes almost the same value. However, there are large differences in $R_{4,1}$, $R_{4,2}$, L_3 and L_4 among the RGA trials. This suggests that the fourth stage in the Cauer circuit is redundant to express the property of the model machine, and q=3 is enough to express the characteristics of this model.

D. Performance of equivalent circuit

The frequency characteristics of the current and losses in steel plate and induction coils obtained by FEA and the equivalent circuit shown in Fig.2 with three stages (q=3) are plotted in Fig. 6. The equivalent circuit has high accuracy for both quantities in the range of interest. In particular, the losses in the steel plate and induction coils are well represented by the equivalent circuit.

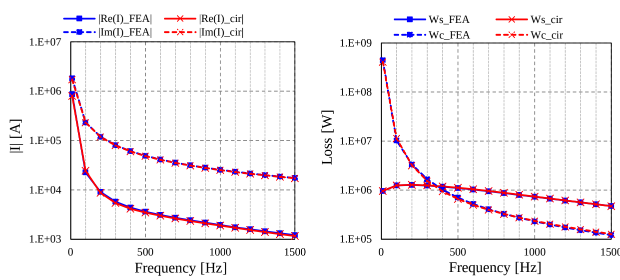

Fig. 6. Frequency characteristics (left: current, right: losses in steel plate and induction coils)

As a useful application of the equivalent circuit, the transient behavior of the current and heating efficiency η which is defined by (15) are evaluated to comparison with conventional FEA.

$$\eta = \frac{W_s}{W_s + W_c} \tag{15}$$

The results are shown in Fig. 7. It can be seen from Fig. 7(a) that the equivalent circuit accurately expresses the transient waveform of the current. Fig.7 (b) shows some discrepancy but good agreement in general. From these results, we expect to predict the transient response of the IH machine with high accuracy in online control using the equivalent circuit. The computing times to compute the frequency and transient responses by FEA and the circuit are summarized in TABLE V. The computing time for the pre-processing to synthesize the equivalent circuit is excluded because our interest is in the use of the equivalent circuit for online control. The proposed method realizes a mathematical model suitable for online control of the IH machines.

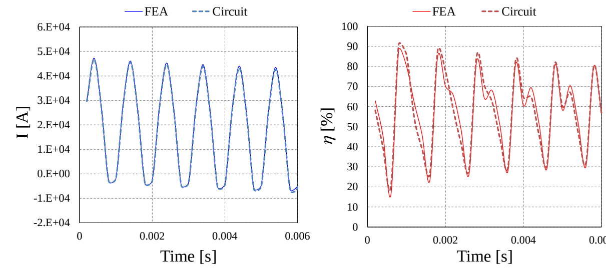

Fig. 7. Transient responses (left: current, right: heating efficiency)

TABLE V COMPUTING TIME

	FEA	Circuit
Frequency response (for 1 freq. sample)	About 50min	Less than 1sec
Transient response (for 1 time step)	About 40min	Less than 1sec

Machine info. Intel(R) Xeon(R) E-2186M CPU@2.90GHz, 64.0GB

IV. CONCLUSION

In this paper, we have proposed a new method to synthesize the equivalent circuit of an IH machine. The proposed method leads to an equivalent circuit which can separately evaluate losses in different components. The circuit parameters are uniquely determined by RGA in conjunction with the regularization method. The equivalent circuit has been shown to have good accuracy. The proposed method would be valid also for electric machines such as transformers and motors.

REFERENCES

[1] O. Lucia, P. Maussion, D. E. J. Burdio, “Induction Heating Technology and its Applications : Past developments, current technology, and future challenges”, *IEEE Trans. Ind. Electron*., vol. 61, no. 5, 2014.
[2] T. Shimotani, Y. Sato, H. Igarashi, “Equivalent-Circuit Generation From Finite-Element Solution Using Proper Orthogonal Decomposition,” *IEEE Trans. Magn.*, vol. 52, no.3, 7206804, 2016.
[3] T. Shimotani, Y. Sato, H. Igarashi, “Direct Synthesis of Equivalent Circuits from Reduced FE Models Using Proper Orthogonal Decomposition,” *The International Journal for Computation and Mathematics in Electrical and Electronic Engineering (COMPEL)*, vol. 35, no. 6, pp. 2035-2044, 2016.
[4] P. Alotto, M. Guarnieri, F. Moro, “A Boundary Integral Formulation on Unstructured Dual Grid for Eddy-Current Analysis in thin shields”, *IEEE Trans. Magn.*, vol. 43, no. 4, pp. 1173-1176, 2007.
[5] J. Smajic, Z. Andjelic, M. Bebendorf, “Fast BEM for Eddy-Current Problems Using H-matrices and Adaptive Cross Approximation”, IEEE *IEEE Trans. Magn.*, vol. 43, no. 4, pp. 1269 -1272, 2007.
[6] D. Schmidthausler, M. Clemens, “Low-Order Electro-quasistatic Field Simulations Based on Proper Orthogonal Decomposition,” *IEEE Trans. Magn.*, vol. 48, no. 2, pp. 567-570, 2012.
[7] P. Dular, F. Henrotte, W. Legros, “A General and Natural Method to Define Circuit Relations Associated with Magnetic Vector Potential Formulations,” *IEEE Trans. Magn.*, vol. 35, no.3, pp. 1630-1633, 1999.
[8] O. Wing, Classical Circuit Theory, Springer, NY, 2010.
[9] Y. Sato, T. Shimotani, H. Igarashi, “Synthesis of Cauer-Equivalent Circuit Based on Model Order Reduction Considering Nonlinear Magnetic Property,” *IEEE Trans. Magn.*, vol. 53, no. 6, 1100204, 2017.
[10] P. C. Hansen, D. P. O’leary, “The use of the L-Curve in the Regularization of discretization of discrete ill-posed problems,” *SIAMJ. Sci. Comput.*, vol. 14, pp. 1487-1503, 1993.